Oxygen and Water Vapor Gas Barrier Poly(ethylene naphthalate) Films by Deposition of SiO_x Plasma Polymers from Mixture of Tetramethoxysilane and Oxygen

N. Inagaki,[1] V. Cech,[2] K. Narushima,[1] Y. Takechi[1]

[1]*Laboratory of Polymer Chemistry, Faculty of Engineering, Shizuoka University, Hamamatsu 432-8561, Japan*
[2]*Institute of Materials Chemistry, Brno University of Technology, CZ-612 00 Brno, Czech Republic*

Received 6 April 2006; accepted 3 November 2006
DOI 10.1002/app.25802
Published online in Wiley InterScience (www.interscience.wiley.com).

ABSTRACT: SiO_x films were deposited from a mixture of tetramethoxysilane (TMOS) and oxygen on poly(ethylene 2,6-naphthalate) film using ion-assisted plasma polymerization technique (Method II) and conventional plasma polymerization technique (Method I), and were compared in chemical composition and gas barrier properties. Methods I and II were different in electrical circuit between electrodes (anode and cathode) and electric power supply. In Method I, the anode electrode was grounded, and the cathode electrode was coupled to the discharge power supply. In Method II, the anode electrode was connected with the discharge power supply, and the cathode electrode was grounded. There was not large difference in SiO_x deposition rate between the plasma polymerizations by Methods I and II. Plasma polymers deposited from $TMOS/O_2$ mixtures by Method II possessed smaller C/Si and O/Si atomic ratios than those deposited by Method I and showed advantage in gas barrier properties. The oxygen and water vapor permeation rates were 0.08–0.13 cm^3 m^{-2} day^{-1} atm^{-1} at 30°C at 90% RH and 0.244–0.276 g m^{-2} day^{-1} at 40°C at 90% RH, respectively. From these results, it can be concluded that the ion-assisted plasma polymerization is a useful technique for deposition of gas barrier SiO_x thin films. © 2007 Wiley Periodicals, Inc. J Appl Polym Sci 104: 915–925, 2007

Key words: oxygen permeation; water vapor permeation; plasma polymerization; XPS; IR spectra; SiO_x

INTRODUCTION

Poly(ethylene 2,6-naphthalate) (PEN) is a kind of polyester, and essentially resembles poly(ethylene terephthalate) (PET) in the physical and chemical properties. PEN as well as PET can be fabricated into biaxially stretched film, which is tough, thermally stable and electrically nonconductive, and transparent in visible light. Therefore, both biaxially stretched PEN and PET films are widely used as base films for transparent electrically conductive indium tin oxide film, flexible printed circuit board, condenser, etc. The performance of the biaxially stretched PEN film is not completely same as that of the biaxially stretched PET film due to contribution of naphthalene ring in the repeating unit. The biaxially stretched PEN films is superior in mechanical and thermal properties to biaxially stretched PET films: Young's modulus for the PEN and PET films (25 μm thickness) is 6080 and 5350 N mm^{-2}, respectively; and glass transition temperature is 121 and 78°C.[1] Especially, biaxially stretched PEN film shows an outstanding feature in the gas barrier properties: the oxygen permeation rate (OPR) through films (25 μm thickness) is 21 and 55 cm^3 m^{-2} day^{-1} atm^{-1} for PEN and PET films, respectively. The water vapor permeation rate (WVPR) is 6.7 and 21.3 g m^{-2} day^{-1}.[1] Therefore, the biaxially stretched PEN film is excellent not only in mechanical and thermal properties but also in gas barrier properties, and is suitable to be used as a raw material for the gas barrier applications such as food and medical packages.

Conventional gas barrier polymeric films involve mainly two types: one is the lamination of a polymer film with excellent gas barrier properties and a base film with tough and chemically stable properties. Poly(vinylidene chloride), poly(vinyl alcohol), ethylene-vinyl alcohol copolymer, and nylon films are commercially used as barrier polymeric materials.[2] Polyolefin films, such as polyethylene and polypropylene, and PET film are widely used as base-film materials. The other type of the gas barrier film is the thin film deposition of metal or ceramic on thermal-resistant polymer film such as PET film. Aluminum is commercially used as metal material for the thin-film deposition, and silicon oxide and

Correspondence to: N. Inagaki (tcninag@ipc.shizuoka.ac.jp).

aluminum oxide also are used as ceramic materials. Recently, mechanically flexible and transparent substrates with excellent gas barrier properties are frequently requested in the field of plastic electronics and optical display applications.[2] Organic light-emitting diode (OLED) display is a typical example of requiring excellent gas barrier films. OPR of less than 10^{-3} cm^3 m^{-2} $day^{-1}atm^{-1}$ and WVPR of less than 10^{-6} $g\,m^{-2}\,day^{-1}$ are required as plastic materials for the application of the OLED display.[3] Many investigators[3–14] have focused on preparation of oxygen and water vapor gas barrier films, and investigated on which thin film is effective in the gas barrier ability and how to deposit the thin film on polymeric film surfaces. Many materials such as SiO_x, SiN_x, AlO_x, AlO_x N_y, diamond-like carbon, etc., have been proposed as barrier materials, and were deposited in a form of thin film of a few hundreds nanometers thickness on polymer film surfaces by plasma polymerization (occasionally called plasma-enhanced chemical vapor deposition) or reactive magnetron sputtering techniques.

SiO_x film is one of effective gas barrier materials, and thin SiO_x film can easily be formed on polymeric film surfaces by plasma-enhanced chemical vapor deposition of organic silane compounds, such as tetraethoxysilane (TEOS), and by sputtering of SiO_2.[4,5,7,9,11,12] The performance of the deposited SiO_x film in the gas barrier properties is related to not only chemistry of the deposited SiO_x film but also morphology of the deposited film.[5,7,15] The SiO_x thin film deposited on polymer surfaces is not dense, but contains some defects in micrometer- and nanometer-size. Many investigators[3–8] believe that such defects in the deposited SiO_x film play a role in reducing the gas barrier performance. How to deposit SiO_x films without such defects on polymer film surfaces is an important subject to demonstrate high performance of gas barrier properties, although chemistry of the deposited SiO_x film also is an essential issue for the high performance.

Which silane compound is used for plasma polymerization is an important factor for the deposition of highly qualified SiO_x films on PEN films. Tetraalkoxysilanes, such as TEOS (boiling point is 169°C at 1.0×10^5 Pa) and tetramethoxysilane (TMOS) (boiling point is 121°C at 1.0×10^5 Pa), are convenient materials for plasma polymerization due to high vapor pressure of these silanes in operating plasma polymerization process at reduced pressures of 10–40 Pa. In the plasma polymerization process, TEOS or TMOS molecules are activated by bombardment of electrons and ions to make bond scission between Si—O, C—O, C—C, and C—H bonds, and as a result, TEOS and TMOS molecules are fragmented into small radicals such as·Si—$(O—CH_2CH_3)_3$ (from TEOS) or ·Si—$(O—CH_3)_3$ (from TMOS),· ·O—Si—$(O—CH_2CH_3)_3$ or ·O—Si—$(O—CH_3)_3$, ·O—CH_2CH_3 or ·O—CH_3, ·CH_2CH_3 or ·CH_3, etc. (fragmentation process). Afterward, such radicals are recombined into larger molecules (recombination process). The repetition of the fragmentation and recombination processes leads to the formation of Si—O network, and at last deposits thin films. Therefore, the deposited thin film is not composed of Si—O component alone, but of a mixture of C—O, C—C, and C—Si components as well as Si—O component. Chemistry of the deposited thin films depends on how to eliminate the carbon components from silane molecules to form Si—O structure in the plasma polymerization process. Inagaki et al.[16,17] investigated the chemistry of plasma polymers deposited from $TEOS/O_2$ and $TMOS/O_2$ mixtures, from viewpoints of XPS spectra, and concluded from the XPS results that $TMOS/O_2$ mixture was one of the successful technologies used to eliminate carbon component from TMOS molecules. Thin films plasma-polymerized from the $TMOS/O_2$ mixtures were mainly composed of Si—O structure, with a small amount of carbon components. Their carbon components were lower in content than those plasma-polymerized from $TEOS/O_2$ mixtures.

How to deposit SiO_x film without defects in micrometer- and nanometer-size on PEN film surfaces also is another important factor for gas barrier materials. Vora and Moravec[18] showed the effects of ion impact on the deposition of diamond-like carbon film from hydrocarbon gases, such as CH_4, C_2H_6, C_3H_8, and C_4H_{10}, using radio-frequency (RF) plasma. Films produced from hydrocarbons by ion-assisted plasma were crystalline. On the other hand, films produced by RF plasma were amorphous. Although the mechanism of the ion assistance toward the deposition of diamond-like carbon film is not yet clear, this ion-assisted plasma technique may be effective in the formation of dense SiO_x films without defects.

From the aforementioned inquiries, we have carried out the plasma polymerization of $TMOS/O_2$ mixtures using ion-assisted plasma to deposit SiO_x films on PEN film surfaces, and investigated the effects of the ion-assisted plasma on the performance of gas barrier properties for SiO_x thin films deposited on PEN film surfaces.

EXPERIMENTAL

Materials

PEN films of 25 μm (Skynex; SKC, Korea[19]) and 100 μm thickness (Teonex; Teijin DuPont Films, Japan[1]), respectively, were used as base substrates for the deposition of SiO_x plasma polymers. The PEN films were washed with ethanol in an ultrasonic washer to remove some contamination from the film surfaces, and were used as base films for the deposi-

TABLE I
Film Properties of Skynex and Teonex

Film name	Film thickness (μm)	Surface roughness (nm)			Gas permeation rate through films	
		R_a	R_{rms}	R_y	O_2[a] ($cm^3\ m^{-2}\ day^{-1}\ atm^{-1}$)	H_2O vapor[b] ($g\ m^{-2}\ day^{-1}$)
Skynex	25	0.84	1.06	9.25	15.1	3.25
Teonex	100	0.76	0.95	6.63	7.36	0.65

[a] At 30°C (90% RH).
[b] At 40°C (90% RH).

tion of SiO_x plasma polymers. Some film properties of Skynex and Teonex are shown in Table I. TMOS purchased from Gelest (Tullytown, PA) was used as a starting material for plasma polymerization of SiO_x.

Reactor used for SiO_x plasma polymerization

A home-made reactor was used for plasma polymerization of SiO_x. The reactor consisted of seven devices: a vacuum chamber (model EBH6, 400 mm diameter, 590 mm high; Ulvac, Japan), a vacuum system with a combination of a rotary pump (320 L min^{-1}) and a diffusion pump (550 L s^{-1}), electric instruments for plasma discharge (electric power supply and diode planar electrodes; model RFG-200; Samco, Japan), flow controllers for TMSO vapor and oxygen gas [metering bellow valve (model BM-4BMG; Nupro, Willoughby, OH) and mass flow controllers (model SEC-400 MARK3; Stec, Japan)], a reeling machine for forwarding PEN films, a thickness monitor for monitoring the SiO_x plasma polymer deposition rate (model CRTM-1000; Ulvac, Japan), and a pressure gauge.

A schema of the plasma reactor used for SiO_x plasma polymerization in this study is shown in Figure 1(a,b). Two different discharge systems with respect to the electric connection between the diode planar electrodes and the discharge power supply were used for the plasma polymerization of the $TMOS/O_2$ mixtures. In the Method I, the anode electrode was grounded, and the cathode electrode was connected with the discharge power supply. In the Method II, the anode electrode was connected with the discharge power supply, and the cathode electrode was grounded. The Method I has been conventionally used for surface modification of organic

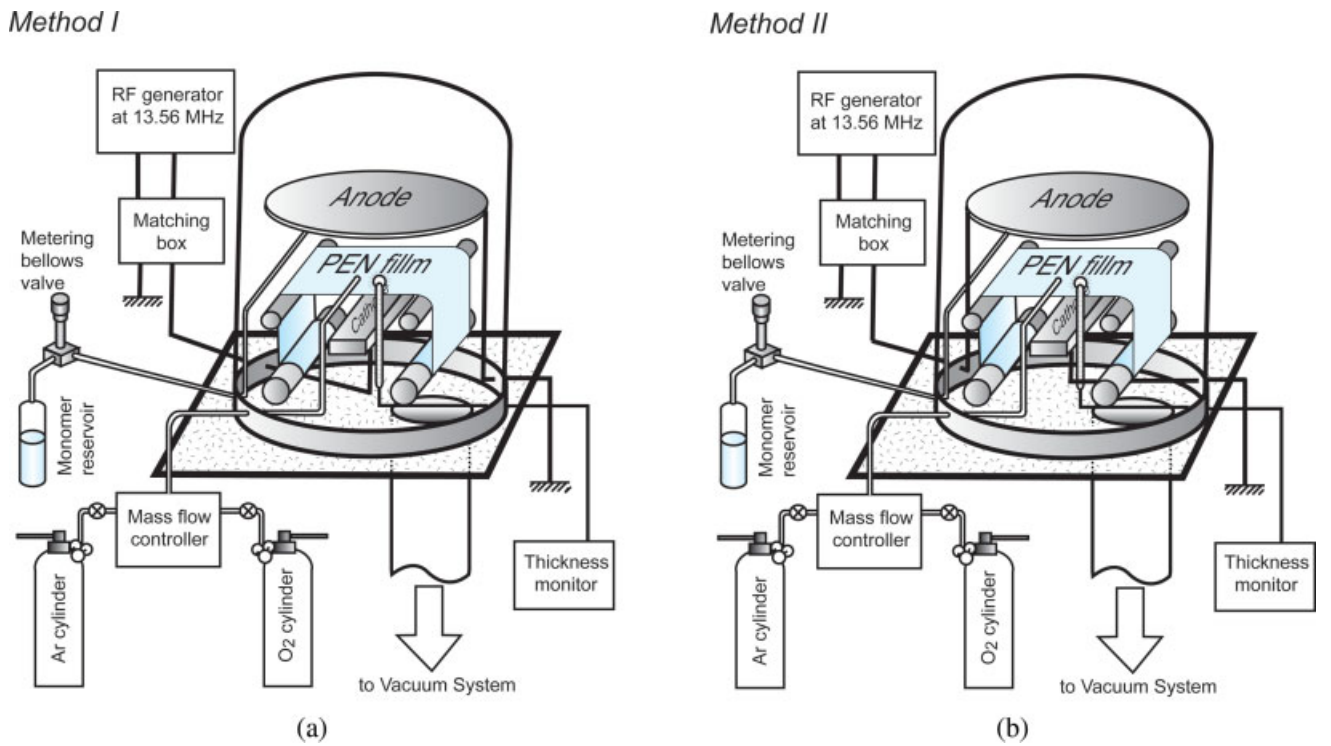

Figure 1 (a) Schema of plasma reactor used for Method I. (b) Schema of plasma reactor used for Method II. [Color figure can be viewed in the online issue, which is available at www.interscience.wiley.com.]

materials (plasma treatment) and the plasma polymerization of organic compounds. On the other hand, the Method II has been used as a special system for the deposition of hard thin films such as diamond-like carbon, titanium nitride, etc. Ion-assisted effects will be expected in the Method II.

Deposition of SiO_x films on PEN film surfaces by plasma polymerization of TMOS/O_2 mixtures

The PEN (110 mm wide × 500 mm long) was set up midway between the anode and cathode in the plasma reactor, and was set up on reels of the rolling machine. TMOS was poured in a reservoir, and air dissolved in the TMOS was removed by a repeated freeze-thaw procedure. Air in the reaction chamber was displaced with argon, and the reaction chamber was evacuated to ~ 0.13 Pa. Afterwards, a mixture of TMOS vapor and oxygen was introduced from the inlet into the reaction chamber. The flow rate of the TMOS vapor and oxygen was adjusted to a given flow rate (1.5–15 cm^3 min^{-1}) by the metering valve and the mass flow controller, respectively. The total flow rate of the TMOS and oxygen was a constant 15 cm^3 min^{-1}. The plasma polymerization of the TMOS/O_2 mixtures was done at a system pressure of 39.9 Pa at RF powers of 30–170 W. The deposition rate of SiO_x plasma films deposited on the PEN films was always monitored by the thickness monitor. At the SiO_x film deposition of 200 nm thickness, the SiO_x plasma polymerization was completed, and the PEN film was taken out from the reaction chamber, and stored in desiccator under silica gel, until the oxygen and water vapor permeation experiments.

IR spectra of the deposited SiO_x films

IR spectra for SiO_x films (~ 200 nm thickness) deposited on the PEN films were measured in a mode of attenuated total reflectance using a universal ATR attachment with a diamond prism (reflective index = 2.4) (PerkinElmer, Yokohama, Japan). A Fourier infrared spectrometer of the Spectrum One (PerkinElmer) was used for the measurement of the IR spectra. The spectra were scanned 32 times in wave number ranges of 4000–680 cm^{-1} at a resolution of 4 cm^{-1}. The analytical depth (d_p) for the ATR-IR spectra was estimated from eq. (1) to be 0.4–2.5 μm in wave number ranges of 4000–700 cm^{-1}.

$$d_p = \frac{\lambda}{2\pi\left[\sin^2\theta - (n_{21})^2\right]^{1/2}} \quad (1)$$

where λ is the wave length of infrared light, θ is the incident angle of the infrared light (45°), and n_{12} is a reflective index ratio of the diamond prism (the reflective index = 2.4) and the deposited SiO_x films (the reflective index of the deposited SiO_x films was assumed to be 1.5). Therefore, the ATR-IR spectra contain not only the deposited SiO_x films but also the PEN films. Differential spectra between the ATR-IR spectra for the deposited SiO_x film and PEN film were obtained using a computer program supplied by Perkin-Elmer to extract the absorption spectra due to the deposited SiO_x film alone.

XPS spectra of the deposited SiO_x films

XPS (C1s, Si2p, and O1s) spectra were obtained on an ESCA 3400 (Shimadzu, Japan) using a Mg Kα photon source. The anode voltage was 12 kV, the anode current was 20 mA, and the background pressure in the analytical chamber was 5×10^{-6} Pa. The C1s, Si2p, and O1s spectra were not smoothed, and the atomic composition of the deposited SiO_x plasma polymer films was calculated from the relative intensity of the C1s, Si2p, and O1s spectra. In the calculation, the sensitivity factors (S) for the C1s, Si2p, and O1s core levels were S(C1s) = 1.00, S(Si2p) = 0.87, and S(O1s) = 2.85, respectively. The C1s spectra were decomposed into four components by a nonlinear, least-squares curve-fitting program supplied by Shimadzu.

Surface topography of deposited SiO_x films

SiO_x films deposited on the PEN films were scanned with a scanning probe microscope (SPM) (SPM-9500; Shimadzu) to evaluate changes in the surface topography by the SiO_x deposition. A silicon cantilever with tetrahedral tip (; Olympus, Japan) was used for SPM image measurements. An area of 1×1 μm^2 on the SiO_x-deposited PEN film surfaces was scanned in a tapping mode, and three parameters, R_a, R_{rms}, and R_y, which meant the average of surface roughness, the root mean square of surface roughness, and the maximum distance between the top and valley of the roughness, respectively, were estimated from the SPM images. R_a, R_{rms}, and R_y parameters were determined from three measurements.

OPR through SiO_x-deposited PEN films

The OPR (in cm^3 m^{-2} day^{-1} atm^{-1}) through the SiO_x-deposited PEN films (area of 78 mm diameter) was measured in ranges of temperature from 10 to 40°C and at a relative humidity of 90% RH using an oxygen barrier tester (model OX-TRAN 2/20; Mocon, Minneapolis, MN). The film specimen was set up in the gas barrier tester, and exposed to oxygen flow at the given temperature for 24 h to do conditioning of the film to the given atmosphere.

TABLE II
Deposition Rate of SiO_x Films

SiO_x deposition conditions		Deposition rate of SiO_x films (nm min^{-1})	
RF power (W)	O_2 concentration in TMOS/O_2 mixture (%)	Method I	Method II
60	0	3.09	–
60	20	–	2.31
60	40	4.51	7.38
60	60	7.05	7.15
60	80	5.77	6.67

Method I: anode electrode was grounded; Method II: cathode electrode was grounded.

Afterward, the oxygen permeation measurement was done four times. The permeation data in the first run was discarded, and the data in the second, third, and fourth runs were averaged.

WVPR through SiO_x-deposited PEN films

The same specimens, as used for the measurement of OPR, were used for the measurement of WVPR. The WVPR through the SiO_x-deposited PEN film was measured with a wet gas water vapor permeability analysis system GTR-100XASU (GTR Tec Corp., Japan) at a relative humidity of 90% RH in the ranges of 25–40°C.

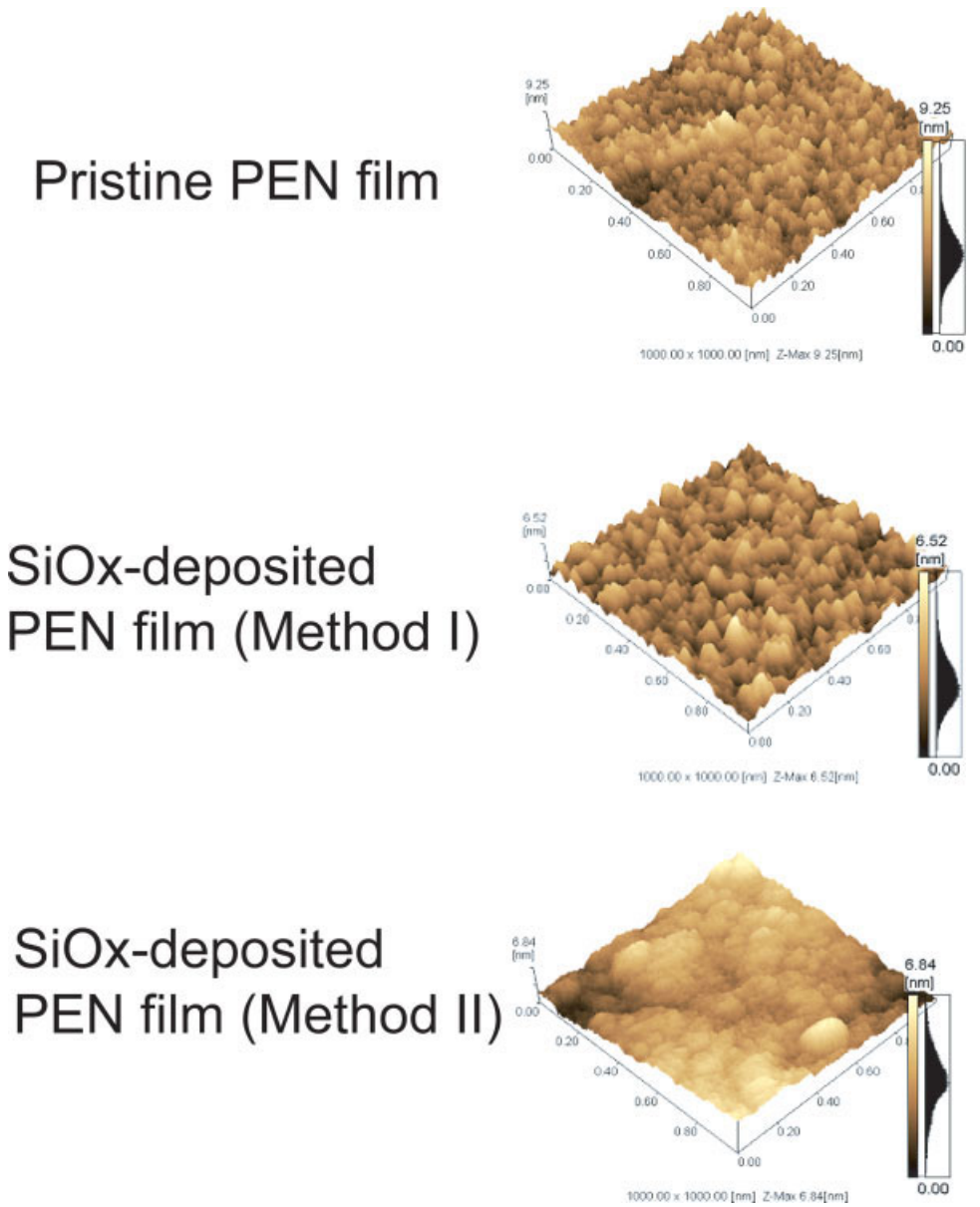

Figure 2 SPM images for SiO_x-deposited PEN films. [Color figure can be viewed in the online issue, which is available at www.interscience.wiley.com.]

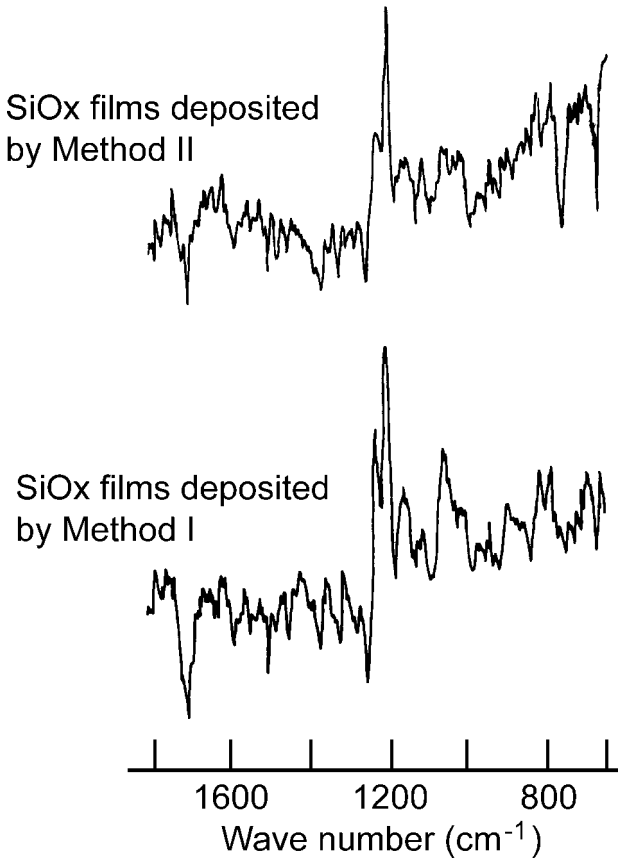

Figure 3 Differential IR spectra for SiO_x films deposited by Methods I and II.

RESULTS AND DISCUSSION

Effects of ion-assisted plasma on deposition and chemistry of deposited SiO_x films

Effects of the ion-assisted plasma were investigated from viewpoints of the SiO_x deposition rate, surface topography of the SiO_x thin films deposited on PEN film surfaces, and chemistry of the deposited SiO_x thin films. Table II compares the deposition rates of SiO_x films in the Methods I and II for the plasma polymerizations of the TMOS/O_2 mixture. The plasma polymerizations were operated at an RF power of 60 W as a function of the oxygen concentration in the TMOS/O_2 mixtures. For example, the deposition rate at an oxygen concentration of 60% was 7.05 and 7.15 nm min^{-1} in the Methods I and II, respectively. Therefore, there was not large difference in the SiO_x deposition rate between the plasma polymerizations in the Methods I and II, except for the plasma polymerization at an oxygen concentration of 40% in the TMOS/O_2 mixtures. Furthermore, the topography of the SiO_x films deposited by the Methods I and II was observed with a SPM. Typical SPM images of the SiO_x films deposited from the TMOS/O_2 mixtures at an oxygen concentration of 60% on PEN (Skynex) film surfaces are shown in Figure 2. The pristine PEN film surface, shown in Figure 3, was covered over with innumerable peaked prominences, and the maximum distance (R_y) between the top and valley of the peaked prominences was 9.25 nm, which is written in the SPM image (Fig. 2). The SiO_x-deposited PEN film surfaces by the Methods I and II also, as shown in Figure 2, showed prominences all over the surfaces, but the shape and size of the prominences were not similar to those of the prominences on the pristine PEN film surface. The prominences of the SiO_x deposited by Method I were gimlet-shaped, which was similar to that of the pristine PEN film surface. On the other hand, the prominences of the SiO_x deposited by Method II were not gimlet-shaped but roundish. This difference in the shape of the prominences may be due to the ion-assisted effects by the Method II. These topographies were evaluated by three parameters, R_a, R_{rms}, and R_y (Table III). There was not a large difference in R_a, R_{rms}, and R_y values between the SiO_x films deposited by the Methods I and II, although the shape of the prominences of the deposited SiO_x films was completely different from each other.

The difference in chemistry between the SiO_x films deposited by the Methods I and II was investigated from the atomic composition. Table IV shows C/Si and O/Si atomic ratios for the SiO_x films deposited by the Methods I and II. Despite exception, the SiO_x

TABLE III
Surface Roughness of SiO_x Deposited on Skynex Films

SiO_x deposition conditions		Surface roughness (nm)					
		R_a		R_{rms}		R_y	
RF power (W)	O_2 concentration in TMOS/O_2 mixtures (%)	Method I	Method II	Method I	Method II	Method I	Method II
60	0	0.334	–	0.421	–	3.223	–
60	20	–	0.455	–	0.576	–	4.542
60	40	0.437	0.396	0.551	0.493	3.856	3.584
60	60	0.643	0.804	0.807	1.036	6.524	6.838
60	80	0.517	0.425	0.656	0.544	5.599	4.216
	Pristine PEN (Skynex)	0.839	0.839	1.059	1.059	9.251	9.251

Method I: anode electrode was grounded; Method II: cathode electrode was grounded.

TABLE IV
Atomic Composition for Deposited SiO_x Films

SiO_x deposition conditions		Atomic composition of deposited SiO_x films			
		C/Si atomic ratio		O/Si atomic ratio	
RF power (W)	O_2 concentration in TMOS/O_2 mixture (%)	Method I	Method II	Method I	Method II
60	0	1.91	–	2.90	–
60	20	0.27	0.37	2.13	1.94
60	40	0.41	0.45	2.41	2.13
60	60	0.64	0.32	2.53	2.17
60	80	0.35	0.20	2.23	2.13

Method I: anode electrode was grounded; Method II: cathode electrode was grounded.

films deposited by Method I possessed higher C/Si and O/Si atomic ratios than those deposited by Method II. For example, the C/Si and O/Si atomic ratios were 0.64 and 2.53 for the SiO_x film deposited from a TMOS/O_2 mixture containing an oxygen concentration of 60% by the Method I. On the other hand, their ratios were 0.32 and 2.17 for the film deposited by the Method II. These SiO_x films deposited by the Methods I and II showed characteristic absorptions due to Si—O—Si, Si—O—CH_3, Si—CH_3 groups, etc., in the IR spectra. Figure 3 shows typical IR spectra for the SiO_x films deposited from a TMOS/O_2 mixture containing an oxygen concentration of 60% by the Methods I and II. These IR spectra were scanned in a mode of attenuated total reflectance, and were differential spectra between the SiO_x film deposited on the PEN film and the pristine PEN film alone, because the analytical depth (d_p) for the ATR-IR spectra measurement exceeded the SiO_x film thickness (200 nm). The d_p depth was estimated from the eq. (1) to be 0.4–2.5 μm in wave number ranges of 4000–700 cm^{-1}. The absorption at 1709 cm^{-1} due to carbonyl groups in ester groups of PEN films was used as a datum point in the differential procedure of two IR spectra. The differential IR spectra for the SiO_x films deposited by the Methods I and II, as shown in Figure 3, resembled each other in absorption peak: strong absorptions appeared at 1230 (Si—CH_3 deformation), 1200 (Si—$(CH_2)_n$—CH_3), 1160 (C—O—C stretching), 1110 (Si—O—Si stretching), 1060 (Si—O—Si stretching), 938 (Si—OH deformation), and 814 cm^{-1} (Si—CH_3 stretching).[20] These absorptions indicate that there was no difference in IR absorption between the SiO_x thin films deposited by the Methods I and II, and those SiO_x films were composed of many components such as Si—CH_3, C—O—C, Si—OH, as well as Si—O—Si groups.

XPS (C1s, Si2p, and O1s) spectra also showed the chemistry of the deposited SiO_x thin films. Figure 4 shows typical XPS spectra for the SiO_x films deposited from the TMOS/O_2 mixture containing 60% O_2 by the Methods I and II. The C1s spectra appeared in a shape of asymmetrical distribution, and the full width at half-maximum (FWHM) value was 3.3 and 2.4 eV for the SiO_x films deposited by the Methods I and II, respectively. These spectra were decomposed into four components, which appeared at 283.5–283.6 eV due to C—Si groups, at 285.0 eV due to CH—CH_2 and CH_2—CH_2 groups, at 286.1–286.2 eV due to C—O groups, and at 287.0–287.5 eV due to C=O groups.[21–24] The relative concentration of these C1s components is listed in Table V. Although the SiO_x film deposited by the Method I, as shown in Table III, possessed larger C/Si atomic ratio than that deposited by the Method II, the C1s spectrum for the SiO_x-deposited film by the Method I comprised the same four components as the C1s spectrum for the SiO_x-deposited film by the Method II. Furthermore, there was not large difference in the relative concentration of the components between the SiO_x-deposited films by the Methods I and II. From these C1s spectra, we believe that the carbon-containing components in the SiO_x-deposited films are mainly C—Si and CH—CH_2 or CH_2—CH_2 groups, which are 77–84% of the total of carbon atoms. On the other hand, the Si2p and O1s spectra, as shown in Figure 4, distributed symmetrically, and their FWHM values were 1.8 and 1.7 eV for the Si2p

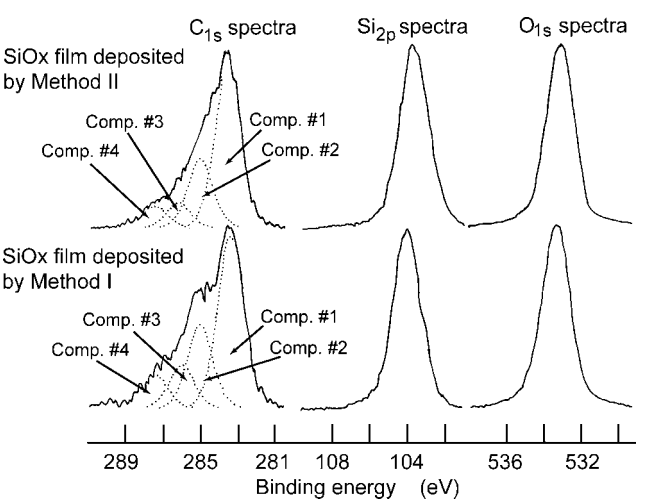

Figure 4 C1s, Si2p, and O1s spectra for SiO_x films deposited by Methods I and II.

TABLE V
XPS Spectra for SiO_x Films Deposited from TMOS/O_2 Mixture Containing 60% O_2 by Methods I and II

Deposition method	Oxygen concentration in TMOS/O_2 mixture (%)	C/Si atomic ratio	C1s spectra (%)				Si2p spectra peak position (eV)	O1s spectra peak position (eV)
			C—Si	CH_2—CH_2 and CH—CH_2	C—O	C=O		
Method I	60	0.64	52	25	13	10	103.9	533.8
Method II	60	0.32	59	25	9	7	103.5	532.8

Method I: anode electrode was grounded; Method II: cathode electrode was grounded.

and O1s spectra, respectively. The symmetrical distribution and small FWHM value of these Si2p and O1s spectra suggest that silicone- and oxygen-containing components were not complex but of simple chemistry. It is well known that the oxidation state of the Si atoms makes binding energy shift of Si2p spectra: Si (oxidation = 0) appears at 99.40 eV, SiO (oxidation = 1) at 100.40 eV, and SiO_2 (oxidation = 2) at 103.25 eV.[25,26] From this reference, we believe that a great portion of Si atoms in the deposited SiO_x films is in the fully oxidized species, SiO_2. This conclusion does not exclude the presence of Si—C component in a small amount in the deposited SiO_x films. Si—CH_3 species was observed in the IR spectra for the deposited SiO_x films (Fig. 3), and Si—C component appeared on the C1s spectra (Fig. 4). The O1s spectra appearing at 532.8–533.3 eV (Fig. 4) also correspond to O1s binding energy for silicon oxide.

From these results, we can conclude the chemical composition for the SiO_x films deposited by the Methods I and II as follows:

1. Plasma polymer films deposited from the TMOS/O_2 mixtures by the Method I possessed higher C/Si and O/Si atomic ratios than those deposited by the Method II.
2. From viewpoints of IR and XPS spectra, there was not large difference between the plasma polymer films deposited from the TMOS/O_2 mixtures by the Methods I and II. The plasma polymer films were composed of components of Si—CH3, C—O—C, Si—OH, as well as Si—O—Si groups.

Gas barrier properties of SiO_x-deposited PEN films

SiO_x films of 200 nm thickness were deposited on the PEN (Skynex) film surfaces, and the OPR through the SiO_x-deposited PEN films was measured at 30°C at a relative humidity of 90% (Table VI). The SiO_x deposition on the PEN films led to great decreases in OPR from 15.1 to 0.45–0.08 $cm^3\ m^{-2}\ day^{-1}\ atm^{-1}$. It is obvious that the SiO_x deposition played a powerful role in improving the oxygen gas barrier properties. The SiO_x deposition by Method II was more advantageous to improving the gas barrier properties than the deposition by Method I. For example, the OPR was 0.18 and 0.08 $cm^3\ m^{-2}\ day^{-1}\ atm^{-1}$ for the SiO_x deposition from the TMOS/O_2 mixtures containing 40% O_2 by the Methods I and II, respectively. Tropsha and Harvey[5] showed an empirical model for the oxygen permeation through SiO_x films deposited on PET film surfaces. Their model is based on the flowing assumptions: (1) the deposited SiO_x films contain many defects of sizes from micrometer-scale to nano-scale. Such defects are traveling channels of oxygen molecules, and the size of these channels plays an important role in permeation process. (2) If the size of the defects is a few hundreds micrometers-scale, oxygen molecules can

TABLE VI
Oxygen Permeation Rate Through SiO_x-Deposited PEN Films (25 μm Thickness)

SiO_x deposition conditions		Oxygen permeation rate[a] ($cm^3\ m^{-2}\ day^{-1}\ atm^{-1}$)	
RF power (W)	O_2 concentration in TMOS/O_2 mixture (%)	Method I	Method II
60	20	–	0.09
60	40	0.18	0.08
60	60	0.45	0.10
60	80	0.17	0.13
Pristine PEN (Skynex)		15.1	15.1

Method I: anode electrode was grounded; Method II: cathode electrode was grounded.
[a] At 30°C (90% RH).

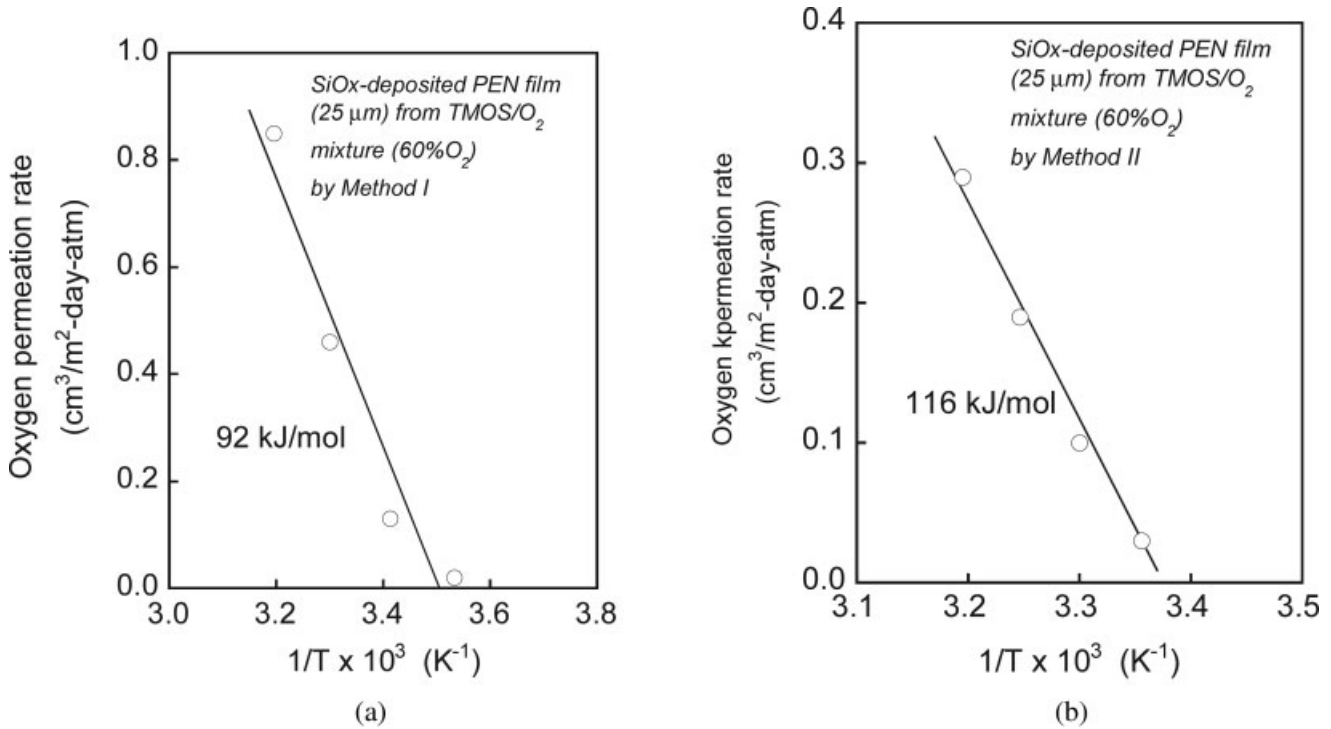

Figure 5 (a) OPR through SiO_x-deposited PEN film (25 μm thickness) by Method I as a function of reciprocal absolute temperature. (b) OPR through SiO_x-deposited PEN film (25 μm thickness) by Method II as a function of reciprocal absolute temperature.

travel the channel of the defects without any obstruction, and traverse PET matrices. As a result, apparent activation energy for the permeation process through the SiO_x-deposited PET films should be equivalent to that for traversing the PET film alone. (3) If the size of the defects is a few nano-scales, oxygen molecules must traverse pinholes of the defects and PET matrices. As a result, apparent activation energy for the permeation process should be a reflex of the structure of the deposited SiO_x films, and may be higher (84–293 kJ mol^{-1}) than that for traversing the PET film alone. Erlat et al.[3,7,8] have applied the empirical model for oxygen and water vapor permeation processes through Al_xO_y- and AlO_xN_y-deposited PET films, and discussed on defects in the deposited Al_xO_y and AlO_xN_y films. Figure 5(a,b) shows effects of temperature (10–40°C) on the OPR through SiO_x-deposited PEN films. In Figure 5(a), the SiO_x-deposited PEN (Skynex) film, which was formed from the $TMOS/O_2$ mixture containing 60% O_2 at a RF power of 60 W by the Method I, was used as a specimen for the oxygen permeation measurement; and in Figure 5(b), the SiO_x-deposited PEN (Skynex) film, which was formed from the $TMOS/O_2$ mixture containing 60% O_2 at a RF power of 60 W by the Method II, was used. The OPR, as shown in Figure

TABLE VII
Water Vapor Permeation Rate Through SiO_x-Deposited PEN Films (25 μm Thickness)

SiO_x deposition conditions		Water vapor permeation rate[a]	Oxygen permeation rate[b]
RF power (W)	O_2 concentration in $TMOS/O_2$ mixture (%)	(g m^{-2} day^{-1})	(cm^3 m^{-2} day^{-1} atm^{-1})
60	20	1.76	0.09
60	40	1.71	0.08
60	60	1.54	0.10
60	80	1.25	0.13
60	90	1.26	0.10
Pristine PEN (Skynex)		3.25	15.1

Method II was used for deposition of SiO_x films.
[a] At 40°C (90% RH).
[b] At 30°C (90% RH).

5(a,b), was a linear relationship with the reciprocal of the absolute temperature. From the slope of the linear relationship, apparent activation energy for traversing the SiO_x-deposited PEN films was estimated. The apparent activation energy was 92 and 116 kJ mol^{-1} for the SiO_x-deposited PEN films by the Methods I and II, respectively. The PEN film as a base film showed an activation energy of 38.5 kJ mol^{-1}. This comparison indicates that (1) the SiO_x films deposited on the PEN film surfaces, irrespective of either Method I or II used for SiO_x deposition, could contribute to oxygen barrier, and (2) there were some differences in nano-scale structure of the defects between the SiO_x deposition by the Methods I and II, and (3) the SiO_x film deposited by Method II was more advantageous in oxygen gas barrier abilities than that by Method I. Which defects in nano-scale structure exist in the deposited SiO_x thin films is not yet interpreted, but the SiO_x thin films deposited by the Method II is preferable for a oxygen barrier material.

The WVPR through the SiO_x-deposited PEN films was measured at 40°C at a relative humidity of 90% (Table VII). The specimens used for the WVPR measurement were the same as those used for the OPR measurement. Table VII shows that the SiO_x deposition by the Method II led to some decrease in WVPR, but the decrement was much less than our expectation. WVPR for the pristine PEN and SiO_x-deposited PEN films was 3.25 and 1.26–1.76 g m^{-2} day^{-1}, respectively. The SiO_x deposition, as shown in Table VII, resulted in great decreases in OPR from 15.1 to 0.08–0.13 cm^3 m^{-2} day^{-1} atm^{-1}, but small decreases in WVPR from 3.25 to 1.26–1.76 g m^{-2} day^{-1}. This comparison between OPR and WVPR indicates that the SiO_x deposition is greatly effective in obstructing the oxygen permeation, but is less effective in retarding the water vapor permeation. This difference may be due to the mechanism of the traveling nano-scale defects in the deposited SiO_x films. As described by Erlat et al.,[3,7,8] oxygen molecules travel freely through defects in the deposited SiO_x films; on the other hand, water vapor molecules may interact and absorb on walls of the nano-scale defects, and surface diffusion of the water vapor molecules may operate on the walls to contribute to WVPR. Detailed nono-scale analysis is necessary to understand the mechanism of traversing the SiO_x-deposited films.

Finally, to improve the water vapor barrier properties, thicker PEN base film was used for deposition of SiO_x: The PEN film thickness was changed from 25 μm (Skynex) to 100 μm (Teonex). The WVPR value for the PEN film of 100 μm thickness (Teonex) was 0.650 g m^{-2} day^{-1} at 40°C at a relative humidity of 90%, and that for the PEN film of 25 μm thickness (Skynex) was 3.25 g m^{-2} day^{-1}. SiO_x films were deposited at a thickness of 200 nm on the PEN (Teonex) films by the Method II, and WVPR for the SiO_x-deposited PEN films was measured at 40°C at a relative humidity of 90% (Table VIII). The SiO_x-deposited PEN (Teonex) films, when the SiO_x deposition was operated at RF powers of more than 100 W, showed better barrier properties than the SiO_x-deposited PEN (Skynex) films (Table VII). Their WVPR value for the SiO_x-deposited PEN (Teonex, 100 μm thick) films was 0.244–0.276 g m^{-2} day^{-1}, and on the other hand, that for the SiO_x-deposited PEN (Skynex, 25 μm thick) films was 1.26–1.76 g m^{-2} day^{-1}. The SiO_x-deposited PEN (Teonex, 100 μm thick) films showed really good performance in water vapor barrier properties, but how much the deposited SiO_x films contributed to the barrier properties is an important subject to be elucidated in the field of packaging technology.

TABLE VIII
Water Vapor Permeation Rate Through SiO_x-Deposited PEN Films (100 μm Thickness)

SiO_x deposition conditions		Water vapor permeation rate[a] (g m^{-2} day^{-1})
RF power (W)	O_2 concentration in TMOS/O_2 mixture (%)	
60	90	0.507
100	90	0.257
130	90	0.244
170	90	0.276
Pristine PEN (Teonex)		0.650

[a] At 40°C (90% RH).

WVPR for the SiO_x-deposited PEN films was only 2.4–2.7 times less than the WVPR value (0.650) for the pristine PEN film. On the other hand, the OPR for the SiO_x-deposited PEN films, as shown in Table VII, was 116–189 times less than the OPR for the pristine PEN films. This comparison points out an important aspect that (1) the deposited SiO_x films contribute effectively to obstruction of the oxygen permeation, but (2) the SiO_x films hardly contribute effectively to retardation of the water vapor permeation. Erlat et al.[3,8] have tried the modification of defect walls on which water molecules could diffuse to improve the water vapor barrier properties. AlO_xN_y films instead of AlO_x films were deposited on PET films to improve the water vapor barrier properties. WVPR for the AlO_xN_y-deposited PET film was 0.11 g m^{-2} day^{-1}, and WVPR for the AlO_x-deposited PET film was 0.42 g m^{-2} day^{-1}. Although the introduction of nitrogen component into AlO_x films could barely improve the water vapor barrier properties, the contribution was not effective. To make breakthrough in the water vapor barrier properties, detailed nono-scale analysis and understanding the mechanism of traversing the SiO_x-deposited

films are necessary. We will do such investigations for technical innovation of water vapor barrier properties.

CONCLUSIONS

SiO_x thin films were deposited using ion-assisted plasma polymerization of a mixture of TMOS and oxygen on PEN film surfaces, and oxygen and WVPRs through the SiO_x/PEN composite films were evaluated to investigate the effects of the ion-assisted plasma on SiO_x deposition. To investigate the effects of the ion-assisted plasma, two electric circuits for plasma discharge (Methods I and II) were used. In the Method I, the anode electrode was grounded, and the cathode electrode was connected with the discharge power supply. In the Method II, the anode electrode was connected with the discharge power supply, and the cathode electrode was grounded. Results are summarized as follows.

1. There was not large difference in the SiO_x deposition rate between the plasma polymerizations in the Methods I and II.
2. The SiO_x films deposited by the Methods I and II showed similar R_a, R_{rms}, and R_y values, although the shape of the prominences of the deposited SiO_x films was completely different from each other; gimlet-shaped for the SiO_x films deposited by the Method I, and roundish for the SiO_x films deposited by the Method II.
3. Plasma polymer films deposited from the TMOS/O_2 mixtures by the Method I possessed higher C/Si and O/Si atomic ratios than those deposited by the Method II.
4. From viewpoints of IR and XPS spectra, there was not large difference between the plasma polymer films deposited from the TMOS/O_2 mixtures by the Methods I and II. The plasma polymer films were composed of components of Si—CH_3, C—O—C, Si—OH, as well as Si—O—Si groups.
5. The SiO_x deposition on the PEN films led to great decreases in OPR from 15.1 to 0.45–0.08 $cm^3\ m^{-2}\ day^{-1}\ atm^{-1}$ at 30°C at 90% RH. The SiO_x deposition by the Method II was more advantageous to improving the gas barrier properties than the deposition by the Method I.
6. The SiO_x deposition on PEN films led to decrease in WVPR. The WVPR was 0.244–0.276 g $m^{-2}\ day^{-1}$ at 40°C at 90% RH.

From these experimental results, we conclude that the ion-assisted plasma polymerization is a useful technique for SiO_x thin film deposition with good gas barrier properties.

References

1. Teijin DuPont Films, Technical Report. Available at http://www.teijindupontfilms.jp.
2. Leterrier, Y. Prog Mater Sci 2003, 48, 1.
3. Erlart, A. G.; Henry, B. M.; Grovenor, C. R. M.; Briggs, A. G. D.; Chater, R. J. J Phys Chem B 2004, 108, 883.
4. Chatham, H. Surf Coat Technol 1996, 78, 1.
5. Tropsha, Y. G.; Harvey, N. G. J Phys Chem B 1997, 101, 2259.
6. Henry, B. M.; Binelli, F.; Zhao, K.-Y.; Grovenor, C. R. M.; Kolosov, O. V.; Briggs, G. A. D.; Roberts, A. P.; Kumar, R. S.; Howson, R. P. Thin Solid Films 1999, 355/356, 500.
7. Erlat, A. G.; Spontak, R. J.; Clarke, R. P.; Robinson, T. C.; Haaland, P. D.; Tropsha, Y.; Harvey, N. G.; Vogler, E. A. J Phys Chem 1999, 103, 6047.
8. Erlat, A. G.; Henry, B. M.; Ingram, J. J.; Mountain, D. B.; McGuigan, A.; Howson, R. P.; Grovenon, C. R. M.; Briggs, G. A. D.; Tsukahara, Y. Thin Solid Films 2001, 388, 78.
9. Wuu, D. S.; Lo, W. C.; Chang, L. S.; Horng, R. H. Thin Solid Films 2004, 468, 105.
10. Abbas, G. A.; McLaughlin, J. A.; Harkin-Jones, E. Diamond Relat Mater 2004, 13, 1342.
11. Madocks, J.; Rewhinkle, J.; Barton, L. Mater Sci Eng B 2005, 119, 268.
12. Wuu, D. S.; Lo, W. C.; Chiang, C. C.; Lin, H. B.; Chang, L. S.; Horng, R. H.; Huang, C. L.; Gao, Y. J. Surf Coat Technol 2005, 198, 114.
13. Seong, J.-W.; Kim, S.-M.; Choi, D.; Yoon, K. H. Appl Surf Sci 2005, 249, 60.
14. Low, H. Y.; Xu, Y. Appl Surf Sci 2005, 250, 135.
15. Deng, C.-S.; Assender, H. E.; Dinelli, F.; Lolosov, O. V.; Briggs, G. A.; Miyamoato, T.; Tsukahara, Y. J Polym Sci Part B: Polym Phys 2000, 38, 3151.
16. Inagaki, N.; Tasaka, S.; Makino, M. J Appl Polym Sci 1997, 64, 1031.
17. Inagaki, N.; Tasaka, S.; Nakajima, T. J Appl Polym Sci 2000, 78, 2389.
18. Vara, H.; Moravec, T. J. J Appl Phys 1981, 52, 6151.
19. SKC Technical Report. Available at http://www.skc.co.kr/en/products/film/skynex_2.html.
20. Bellamy, L. J. The Infrared Spectra of Complex Molecules; Wiley: New York, 1966.
21. Beamson, G.; Briggs, D. High Resolution XPS of Organic Polymers. The Scienta ESCA 300 Database; Wiley: Chichester, 1992.
22. Zinovev, A. V.; Elam, J. W.; Moore, J. F.; Hryn, J. N.; Auciello, O.; Carlisle, J. A.; Pellin, M. J. Thin Solid Films 2004, 469/470, 135.
23. Seyller, Th.; Graupner, R.; Sieber, N.; Emtsev, K. V.; Ley, L.; Tadish, A.; Riley, J. D.; Leckey, R. C. G. Phys Rev B 2005, 71, 245333.
24. http://srdata.nist.gov/xps
25. Hollinger, G.; Himpsel, F. J. Phys Rev B 1983, 28, 3651.
26. Himpsel, F. J.; McFeely, F. R.; Hollinger, G. Phys Rev B 1988, 38, 6084.